INVESTIGATIONS OF POLLUTANT PREDICTIONS WITH LES-CMC MODELLING IN A BLUFF-BODY STABILIZED NON-PREMIXED FLAME

S. Navarro-Martinez
Department of Mechanical Engineering
Imperial College London
London SW7 2AZ, UK
s.navarro@imperial.ac.uk

A. Kronenburg
Department of Mechanical Engineering
Imperial College London
London SW7 2AZ, UK
a.kronenburg@imperial.ac.uk

W. P. Jones
Department of Mechanical Engineering
Imperial College London
London SW7 2AZ, UK
w.jones@imperial.ac.uk

ABSTRACT

The Large Eddy Simulations (LES)-Conditional Moment Closure (CMC) method is applied to a bluff body stabilized flame. First, computations of the velocity field and mixture fraction are compared with experimental data and the influence of grid size and inflow boundary conditions is analysed. Then, predicted reactive species mass fractions are compared with measurements in conditional and in real space. It can be shown that conventional steady flamelet methods cannot predict accurately intermediate species such as CO and criteria pollutants such as NO and the solution of the unsteady CMC equations is required to predict NO and CO satisfactorily since species mass fraction vary with downstream distance. The quality of NO and CO predictions is comparable to the best existing species predictions of the Sydney bluff-body burner, but temperature is markedly overpredicted close to the nozzle and predicted CO and NO mass fraction are generally somewhat above measurements.

INTRODUCTION

In recent years, relatively simple combustion sub-models that were initially developed for RANS based simulations have been implemented into LES to model the source terms of chemically reacting species. LES can improve the predictive capabilities of the models by providing a better description of the turbulent flow without the a-priori adjustments that are needed in RANS calculations. The progress of LES in reacting flows is, however, limited by the sophistication of the combustion models. LES does not solve the closure problem associated with the chemical source terms since reactions occur at molecular level on the unresolved scales.

The CMC model has performed remarkably well in RANS simulations of non-premixed turbulent flames (Klimenko and Bilger, 1999). CMC is based on the idea that reactive scalar fluctuations conditioned on the mixture fraction (hereafter ξ) are much smaller than unconditional fluctuations and simple first order closure of the non-linear conditionally averaged chemical source term normally yields satisfactory accuracy. The feasibility of using CMC as a combustion sub-model for LES has been demonstrated in Navarro-Martinez *et al.* (2005), where very good agreement between simulation and experiments has been obtained. Predictions of all major species in the piloted Sandia Flame D (Barlow and Frank, 1998) are excellent and NO predictions are clearly superior to RANS based CMC calculations.

Bluff-body stabilized flames constitute a bigger challenge than jet flames. The steady recirculation structures behind the bluff-body create intense mixing of reactants and combustion products and a detailed description of the flow and mixing fields is required for accurate reactive species predictions. The existence of a three shear-layer structure increases the demands on grid resolution and RANS solutions of bluff-body flames are very sensitive to the modelling constants (Muradoglu *et al.* 2003). LES of bluff-body flames by different research groups have shown some variations in the predictions of flow and mixing fields (see proceedings of TNF7 Workshop, 2004). These differences cannot solely be attributed to the combustion model, and turbulent inflow structures seem to affect the flow evolution. Very different flame structures can be obtained with different inflow fluctuations (Esquiva-Dano and Escudie, 2005).

In addition to the increased requirements for the solution of the flow and mixing fields, it can be expected that turbulence-chemistry interactions are more significant in bluff-body flames than in Sandia Flame D and that simple steady

flamelet models will fail to give satisfactory agreement of predicted intermediates and pollutants with measurements. Conditional moments are expected to vary in space and LES-CMC allows for the inclusion of detailed chemistry and a time and space dependent evolution of the conditionally averaged species mass fractions. The LES-CMC approach is computationally more expensive than the steady flamelet approach but its implementation will be necessary for more accurate CO and NO predictions.

In the next Section, the LES-CMC approach is introduced and the major modelling assumptions are explained. Details on the numerical simulation of the bluff-body flame are presented in Section and the following discussion mainly focuses on the mesh dependence of the flow field simulations and the variations of the conditional moments due to different flow and mixing field and their spatial dependence.

MATHEMATICAL MODELLING

The numerical model can be split into two parts, the LES solver where transport equations for the flow field $\tilde{\mathbf{v}}$ and the passive scalar field are solved on a fine LES-grid, and the CMC solver that provides the conditionally filtered mass fractions and enthalpy as functions of time and space. The CMC grid can be much coarser than the LES grid due to the expected relatively weak spatial variations of the conditional moments. The combustion is coupled with the flow field solution through density and molecular viscosity that can be obtained from the equation of state and Wilkes's mixing formula, respectively.

LES Modelling

The Favre filtered Navier-Stokes equations are solved with an in-house finite volume code using a staggered grid arrangement. A two-step integration scheme is combined with central differences for the convective and diffusive parts, while a total variation diminishing (TVD) scheme is used for the discretisation of the convective term in the passive scalar transport equations. TVD schemes are often used in LES of reacting flows to avoid unphysical oscillations in the scalar field. The Smagorinsky model is used for the closure of the subgrid (SGS) contributions and the proportionality constant is obtained from the dynamic procedure suggested by Piomelli and Liu (1995). A gradient-type model approach is used for the subgrid variance, $\widetilde{\xi''^2_{sgs}}$, viz

$$\widetilde{\xi''^2_{sgs}} = C_\xi \Delta^2 \left(\frac{\partial \tilde{\xi}}{\partial x_i} \frac{\partial \tilde{\xi}}{\partial x_i} \right). \tag{1}$$

Here, C_ξ has been chosen to be equal to 0.1 (Branley and Jones 2001). The filtered scalar dissipation $\tilde{\chi}$ can be split into two contributions (discarding inter-scale cross-terms)

$$\tilde{\chi} = 2D \left(\widetilde{\frac{\partial \xi}{\partial x_i} \frac{\partial \xi}{\partial x_i}} \right) = \chi_m + \chi_{sgs}, \tag{2}$$

where sub-grid fluctuations of the diffusion coefficient D are neglected. The variable χ_m is the large scale dissipation which can be directly obtained from the resolved scalar field and χ_{sgs} is the subgrid scalar dissipation. The latter is modelled as

$$\chi_{sgs} = 2D_t \left(\frac{\partial \tilde{\xi}}{\partial x_i} \frac{\partial \tilde{\xi}}{\partial x_i} \right). \tag{3}$$

where D_t is the turbulent diffusivity obtained proportional to the subgrid viscosity using a turbulent Schmidt number of 0.4 (Pitsch and Steiner 1998). It shall be noted that the exact choice of the turbulent Schmidt number does not greatly affect the scalar field solution and results with $Sc_t = 0.7$ show very small differences in axial and radial distribution (results not shown). Inflow boundary conditions are critical in LES simulations and excessive inflow turbulence leads to the prediction of a faster jet decay. In the investigated bluff-body flame, the flame surface is placed in the outer shear layer and the flame is therefore very susceptible to turbulent perturbations in the inflow region. In this work, axial velocity fluctuation are correlated in time and circumferential direction and they are superimposed on the mean velocity profiles. The initial perturbations approximate the mean square fluctuations (RMS) as suggested by Pitsch and Steiner (2000).

Conditional Transport Modelling

A conditional filtering operation of a variable Φ is defined as

$$\overline{\Phi|\eta} \equiv \frac{\int_V \Phi \psi_\eta \left(\xi(\mathbf{x}',t) - \eta\right) G\left(\mathbf{x} - \mathbf{x}', \Delta\right) dV'}{\bar{P}(\eta)} \tag{4}$$

where G is a positive defined space filter with filter width Δ, ψ_η is a fine-grained Probability Density Function (PDF), $\bar{P}(\eta)$ is a subgrid PDF and η is the sample space of mixture fraction, ξ. In variable density flows, conditional density-weighted (Favre) filtering is used, $\bar{\rho}_\eta \tilde{\Phi}_\eta = \overline{\rho\Phi|\eta}$, where tilde denotes Favre filtering and $\tilde{\Phi}_\eta \equiv \widetilde{\Phi|\eta}$ has been introduced. Similarly, the Favre subgrid PDF, $\tilde{P}(\eta)$, can be obtained.

The filtering operation (4) is applied to the transport equation of the reactive scalar, Y_i , and the transport equation for the conditionally filtered mass fractions can then be written as

$$\frac{\partial Q}{\partial t} + \tilde{\mathbf{v}}_\eta \cdot \nabla Q = \tilde{W}_\eta + \frac{\tilde{\chi}_\eta}{2} \frac{\partial^2 Q}{\partial \eta^2} + e_Y + e_D, \tag{5}$$

where $Q \equiv (\tilde{Y}_i)_\eta$ and $\tilde{W}_\eta$ is the conditionally filtered chemical source term. The term

$$e_Y \equiv \frac{1}{\bar{\rho}_\eta \tilde{P}(\eta)} \nabla \cdot \left[\bar{\rho}_\eta \left(\tilde{\mathbf{v}}_\eta Q - \widetilde{(\mathbf{v} Y_i)}_\eta \right) \tilde{P}(\eta) \right] \tag{6}$$

accounts for transport in physical space of the conditional fluctuations and

$$e_D \equiv \frac{1}{\bar{\rho}_\eta \tilde{P}(\eta)} \nabla \cdot \bar{\rho}_\eta \tilde{P}(\eta) \widetilde{(D \nabla Y_i)}_\eta \tag{7}$$

represents transport of the conditional scalar due to molecular diffusion. Interactions between physical and conditional fluctuations have been neglected (Navarro-Martinez *et al.* 2005). The unconditional (LES) and the conditionally filtered (LES-CMC) values are related by

$$\tilde{Y}_i = \int Q \tilde{P}(\eta) d\eta. \tag{8}$$

It is assumed that $\tilde{P}(\eta)$ can be approximated by a two-moment β-PDF. In non-premixed combustion away from extinction, conditional moments change slowly in space and time and grids can be relatively coarse for the solution of the conditionally filtered equations, especially in the cross-stream direction.

Full closure of equations (5) can be achieved by modelling the conditional dissipation, $\tilde{\chi}_\eta \approx < \tilde{\chi} | \eta >$. The modelling is

based on the assumption of local homogeneity of the conditional moments in one CMC cell. A similar process is applied for the modelling of the conditional velocity and details of the closures can be found in Navarro-Martinez *et al.* (2005). The terms e_Y and e_D are modelled using a gradient-type approach similar to RANS-CMC methods, $e_Y \approx -\nabla \cdot (D_\eta \nabla Q)$, where the modelling of D_η is again based on local homogeneity of the conditional moments in one CMC cell.

NUMERICAL SIMULATION

The test case computed here is the Sydney burner configuration HM1, which has been recently studied experimentally (Swaminathan and Dally 1998, Dally *et al.* 2004) and numerically (e.g. Dally *et al.* 1998, Kim and Huh 2002, Liu *et al.* 2005) and has been extensively discussed at the 7th Workshop on Turbulent Diffusion Flames (Proceedings of TNF7, 2004) where several LES and RANS results were presented.

The experimental set-up consists of a central jet of a mixture of CH_4 and H_2 (50:50) with a bulk velocity of 118 m/s. The co-flow is air with a velocity of 40 m/s. The stoichiometric mixture fraction is 0.05, which places the reaction region in the outer shear layer. The jet has a diameter of 3.6 mm while the bluff body has a diameter of $d = 50$mm. The jet Reynolds number is 15,800 and the adiabatic flame temperature is $T_{ad} = 2265$K. The experimental data provide measurements at different axial locations of temperature, of major species, of intermediates such as OH and CO, and of NO concentrations. An equivalent flame, HM1e, was used to obtain the velocity data by LDV (Laser Doppler Velocimetry). HM1e has slightly lower jet and co-flow velocities (108 and 35 m/s respectively). In this work the flame HM1 is computed and therefore slight differences are expected for predictions of the velocity field.

In the present work we have used a 48 species, 300 reactions mechanism (Meyer 2001) to approximate the chemical kinetics of CH_4 combustion. This study focuses on the recirculation and the neck region of the bluff-body flame, where experimental measurements were obtained. Therefore, the current study is limited to the near field region. The domain extends $4d$ and $3d$ in axial and radial direction, respectively.

Table 1 list the different computational grids used in this work. The cylindrical grids (G1 and G2) have finer resolution in radial direction of the shear layers with uniform cell aspect ratios Δ_z/Δ_r which benefit the numerics. Cartesian grids behave better away from the nozzle and they do not required any explicit treatment of the centreline but errors at the inflow occur due to the mapping of a round jet onto a Cartesian mesh. In addition, the resolution of the shear layer requires a much greater number of nodes which increases the computational cost. The computational requirements of the Cartesian grid (GC) are double of those of G2. A complete G1 simulation with statistics sampling after start-up takes 768 processor hours on 2.4 GHz Pentium 4 processors, while G2 requires approximately 3100 CPU hours. The CMC grid in both G1 and G2, consists of 32 nodes in axial direction, 6 nodes in circumferential direction and 60 nodes in mixture fraction space. In mixture fraction space, the grid points are clustered around stoichiometric. The Cartesian grid has 4×4 CMC nodes in the cross stream direction. Statistics are obtained over 50 ms in G1 and 20 ms in G2 and GC. Statistics are taken after a fully turbulent flow has been established and initial transients have been convected downstream to the boundaries of the computational domain.

Table 1: Grid properties. N_{jet} is the number of nodes in radial direction within fuel jet, z is the axial direction

Grid	$N_z \times N_r \times N_\phi$	Δ_x/Δ_r	N_{jet}
G1	$160 \times 80 \times 36$	1.7-4	4
G2	$256 \times 92 \times 48$	1.0-3.7	5
GC	$200 \times 120 \times 120$	0.15-2	4(Cartesian)

RESULTS AND DISCUSSION

Figure 1 shows the instantaneous filtered temperature in the central x-z plane. The predicted flow is fully turbulent after $z/d = 1$, with fine structures generated by the instability of the inner shear layer and large vortices generated by the outer shear-flow. At $z/d = 2$, hot and cold fluid parcels (dark and white areas) are very close and this region is probably intermittent (Kempf *et al.*, 2004)

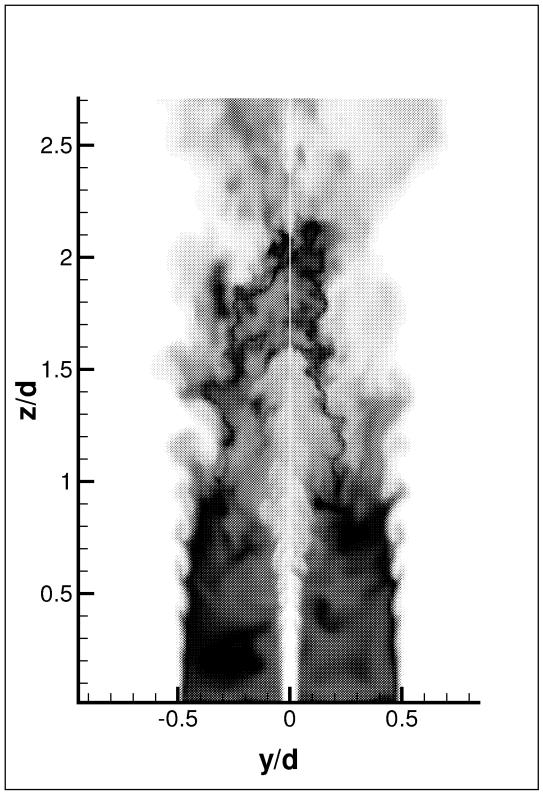

Figure 1: Instantaneous profiles of temperature. Dark grey indicates higher temperature (Grid G2).

Very good agreement is obtained for the jet decay on the centreline when the Cartesian grid is used as shown in Fig. 2. The cylindrical grids predict a somewhat faster decay of the jet, but results improve as the grid is refined. These results are in line with numerical simulations of Kempf *et al.* (2004) and Liu *et al.* (2005) where the centreline mixture fraction is under-predicted in downstream regions. The correct centreline decay seems somewhat fortuitous when using the Cartesian grid since radial mixture fraction profiles clearly

over-predict mixture fraction away from the centreline while the radial mixture fraction distribution is well predicted with the cylindrical grids (Fig 3).

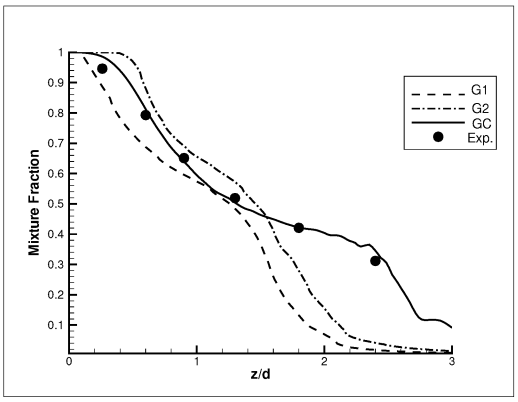

Figure 2: Axial distribution of mean mixture fraction at the centreline for different grids. Symbols indicate experimental measurements

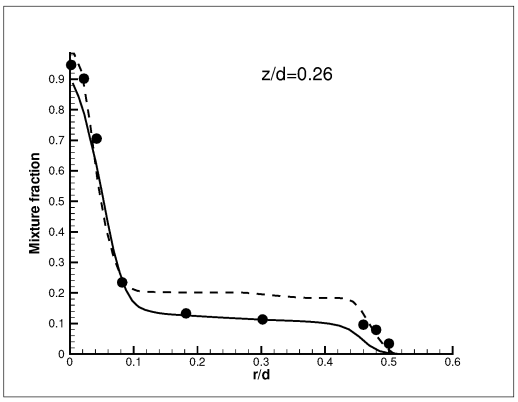

Figure 3: Mixture fraction distribution at $z/d = 0.26$ for the Cartesian (dashed line) and G1 cylindrical grid (solid line).

These findings are largely consistent with existing LES simulations of the bluff-body flame if seen in conjunction with Figs. 4-5. The Cartesian grid clearly underpredicts the turbulent velocity fluctuations and it does not capture the turbulent shear layer well. An essentially laminar shear layer is predicted which may lead to the "correct" flame length. The LES by Raman and Pitsch (Proceedings of TNF7) may be interpreted similarly. In contrast, the more accurate modelling of the turbulence levels in the outer shear layer that can be obtained with grids G1 and G2 lead to shorter recirculation zones and therefore shorter flame lengths. These results are again in line with findings at TNF7 and current modelling efforts could not shed light on the apparent inconsistencies in either the simulations or eventually in the measurements.

The inflow turbulent conditions have a major effect on the jet break-up. The inflow turbulence length scales were chosen to be between one and one eighth of the jet diameter. Figure 6 shows results from computations with laminar and turbulent inflow conditions for G2. Due to turbulence, the jet breaks up earlier, however, the results downstream of $z/d = 1$ are largely unaffected by the inflow conditions, the outer shear layer is always turbulent which leads to the shortened recirculation zones and flame length.

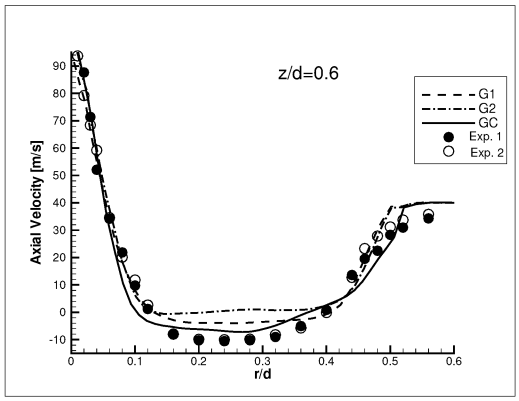

Figure 4: Axial velocity distribution at $z/d = 0.6$ for different grids. The symbols denote two experimental sets of measurements over flame HM1e.

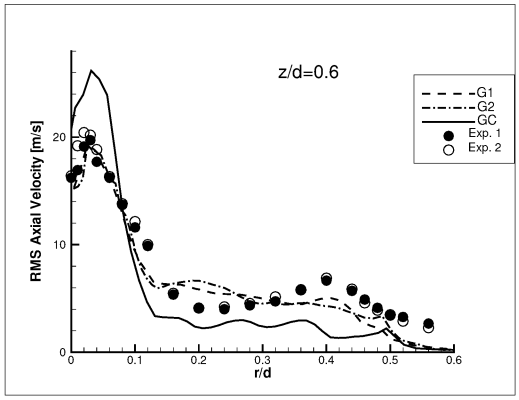

Figure 5: Axial velocity fluctuations distribution at $z/d = 0.6$ for different grids. The symbols denote two experimental sets of measurements over flame HM1e.

The predicted conditional temperature and major reactive species are in satisfactory agreement in the recirculation and neck regions. However, partial extinction may occur and lead to temperature depression close to the nozzle. In addition hot product gases are cooled on the bluff-body surface before mixing with the fresh reactants. Both of these effects cannot be captured by the current model and predictions yield an overprediction of conditional temperature of around 10% close to the nozzle, while the finer grid G2 somewhat improve the results by a few percent.

Figure 7 compares results for the conditionally averaged CO mass fractions from runs G1 and G2 with measurements. Clear improvements in the predictions can be seen when the finer grid is used which results directly from the improved temperature predictions due to better grid resolution. The same is true for predictions of NO. NO formation is thermally controlled and the reduction in peak temperature has a clear effect on NO levels throughout the flow. Lower temperatures and species mass fractions mainly result from increased scalar dissipation in case G2. Hence, the levels of sub-grid scale dissipation do not reflect the "true" value for the grid G1 which highlights the need for either good resolution of the flow and scalar field or for improved subgrid scale models. Fig. 8 demonstrates a relatively minor contribution of the conditional fluctuations to the balance in the conditional moment

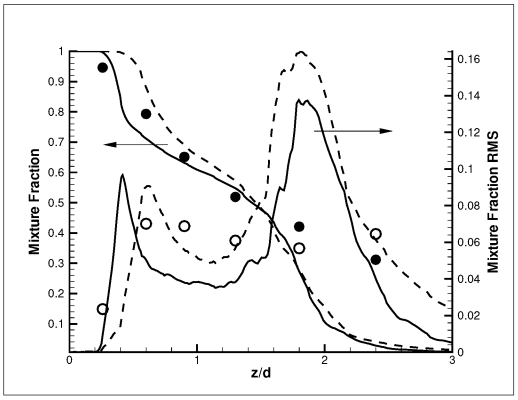

Figure 6: Axial mean and RMS distribution of mixture fraction at the centreline for laminar inflow (dashed line) and turbulent(solid line.) Symbols indicate experimental measurements

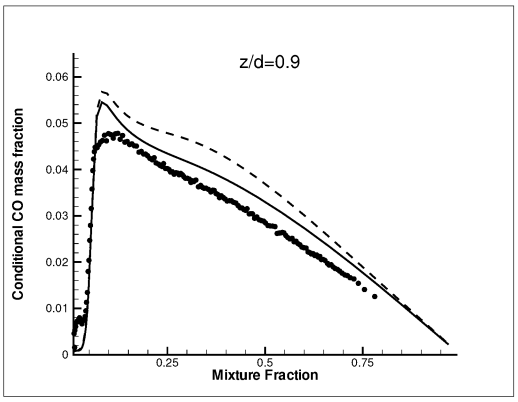

Figure 7: Conditional CO mass fraction distribution at $z/d = 0.9$. G1 (dashed line) and G2 (solid line).

transport equations. Inclusion of the e_Y-term improves CO predictions by less than 5% while RANS-CMC computations show a much larger influence of the fluctuation term on the species mass fractions (Kim and Huh, 2002). It may be concluded that sufficient grid resolution in LES may make the modelling of e_Y unnecessary.

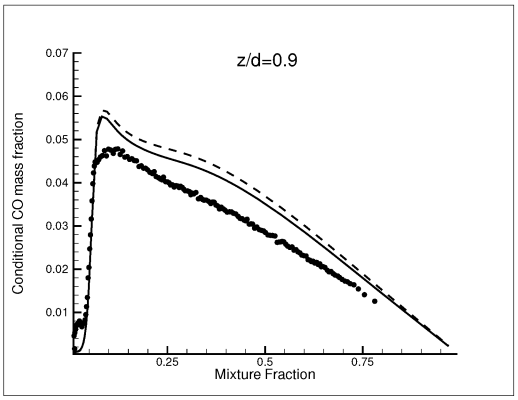

Figure 8: Conditional CO mass fraction distribution at $z/d = 0.9$ (Grid G1), $e_D, e_Y = 0$ (dashed), $e_D, e_Y \neq 0$ (solid).

In Fig. 9 the contributions of the terms in eq. (5) are plotted. The axial convective term $\partial u/\partial z$ is dominant (1-2 orders of magnitude) over the azimuthal contributions $1/r\partial w/\partial\theta$. The relative contribution of angular transport to the CMC transport equation decays as we move downstream. Fig. 9(b) shows that at $z/d = 0.9$ the axial convection term is approximately equal to the sum of the dissipation and chemical source terms on the rich side. All other terms are negligible and changes in conditional mass fractions with downstream distance are due to the balance of the diffusive and reactive terms. Although the conditional angular transport does not seem to have a major effect at $z/d = 0.9$, the introduction of an angular dependence of the conditional moments nodes clearly improves the results. Most species predictions show some improvement and major differences can be seen in Fig. 10 for conditionally averaged NO mass fractions. This improvement is primarily not caused by azimuthal transport but the angular variation of scalar dissipation conserves high peaks in conditional dissipation and directly affects conditional mass fractions (Pitsch and Steiner 2000). On the lean side of the flame, azimuthal conditional transport is more important and must not be neglected for accurate species predictions.

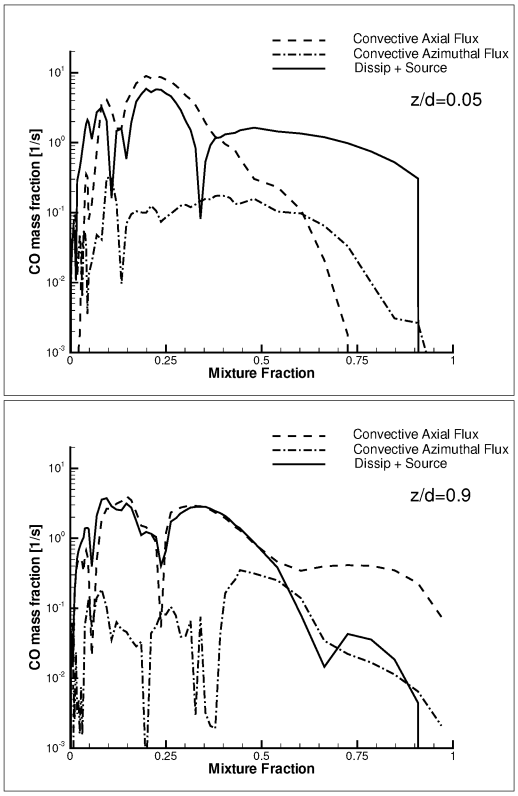

Figure 9: Absolute values of the terms in equation (5) for CO at $z/d = 0.05$ and 0.9 (Grid G1) averaged over 3 ms.

Figure 11 shows radial distributions of NO and CO inside the recirculation region and close to the nozzle. Despite the improvements in the description of turbulent flow due to the use of LES, the results still severely overpredict NO, especially close to the reaction zone ($r/d \approx 0.5$). At this location, a distinct maximum can be observed which is not verified by the experiments. This maximum in the predictions is is caused by low $\widetilde{\xi''^2_{sgs}}$ predictions in the outer shear layer and an overprediction of conditionally averaged NO close to stoichiometric due

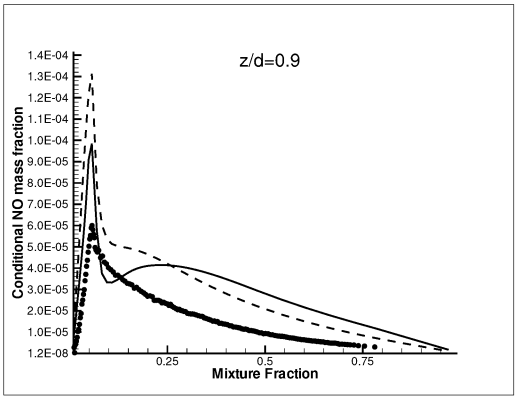

Figure 10: Conditional NO mass fraction distribution at $z/d = 0.9$ without (dashed) and with angular distribution of CMC nodes (solid line).

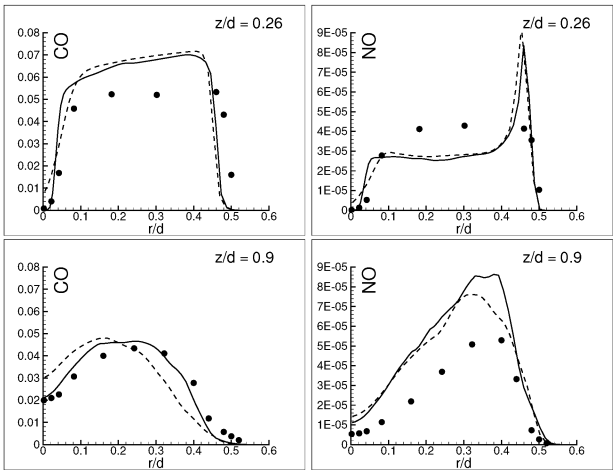

Figure 11: CO (left) and NO (right) mass fractions radial distribution at $z/d = 0.26$ and 0.9. G1 (dashed line) and G2 (solid line).

to overpredicted conditional temperature. CO results show much better agreement with experiments.

CONCLUSIONS

A LES-CMC model has been applied to a bluff-body using first order closure and conventional CMC assumptions. Velocity predictions are generally satisfactory but the flame length is underpredicted. Therefore, only the near field region has been analysed for an assessment of the combustion submodel. Temperature predictions exceed measurements by up to 10% close to the nozzle leading to an artificial excess of CO and NO and to inaccurate species predictions in the outer shear layer. Grid refinement greatly improves the results by better resolution of the scalar gradients in the outer shear layer. This leads to higher scalar dissipation which directly affects conditional mean quantities. The influence of the bluff-body wall has been neglected and heat loss is expected to be responsible for the overpredicted temperatures. Future studies will address this issue.

ACKNOWLEDGEMENTS

The authors wish to acknowledge the financial support from EPSRC under grant number GR/R69792 and from the Imperial College Computing Centre.

REFERENCES

Barlow, R. S. and Frank, J., 1998, "Effects of Turbulence on species mass Fractions in Methane-Air jet flames", *Proc. Comb. Inst.*, Vol. 27, pp. 1087.

Branley, N. and Jones, W. P., 2001, "Large Eddy Simulation of a Turbulent Non-premixed flame", *Combustion and Flame*, Vol. 127, pp. 1914-1934.

Dally, B. B. , Fletcher, D. F. and Masri, A. R., 1998, "Flow and Mixing Fields of Turbulent Bluff-Body Jets and Flames", *Combust. Theory Modelling*, Vol. 2, pp. 193-219.

Esquiva-Dano, I. and Escudie, D., 2005, "A way of considering the influence of the bluff-body geometry on the nonpremixed flame stabilization process", *Combustion and Flame*, to appear.

Kempf, A., Lindstedt, R. P. and Janicka, J., 2004, "Large Eddy Simulation of a Bluff-Body Stabilized Non-Premixed Flame" *Combustion and Flame*, to appear.

Kim, S. H., and Huh, K. Y., 2002, "Use of the Conditional Moment Closure to Predict NO formation in Turbulent CH4/H2 Flame over a Bluff-Body", *Combustion and Flame*, Vol. 130, pp. 94-111.

Klimenko, A. Y. and Bilger, R. W., 1999, "Conditional Moment Closure for Turbulent Combustion", *Progr. Energy Combust. Sci.*, Vol. 25, pp. 595-687.

Liu, K., Pope, S. B. and Caughney, D. A., 2005, "Calculations of Bluff-Body Stabilized Flames using a Joint Probability Density Function Model with Detailed Chemistry", *Combustion and Flame*, to appear.

Meyer, M., 2001, "The application of detailed and systematically reduced chemistry to transient laminar flames", PhD Thesis, Imperial College

Muradoglu, M., Liu, K. and Pope, S. B, 2003, "PDF modelling of a bluff-body stabilized turbulent flame", *Combustion and Flame*, Vol.132, pp 115-137.

Navarro-Martinez, S., Kronenburg, A. and Di Mare, F., 2005, "Conditional Moment Closure for Large Eddy Simulations", *Flow, Turb. and Combustion*, to appear.

Pitsch, H. and Steiner, H., 2000, Large-eddy simulation of a turbulent piloted methane/air *Physics of Fluids*, Vol. 12, Num. 10, pp. 2541-2554.

Piomelli, U. and Liu, J., 1995, "Large-eddy simulation of rotating channel flows using a localized dynamic model", *Physics of Fluids*, Vol. 7, Num. 4, pp. 839-848.

Swaminathan, N. and Dally, B. B., 1998, "Cross Stream Dependence of Conditional Averages in Elliptic Region of Flows behind a Bluff-Body" *Physics of Fluids*, Vol. 10, Num. 9, pp. 2424-2426.

Proceedings of the TNF7 Workshop, 2005 *Proceedings of the 7th Turbulent Non-Premixed Flames Workshop*, http://www.ca.sandia.gov/tdf/Workshop.html